

Molecular Identification of K-Cl Cotransporter in Dog Erythroid Progenitor Cells

Hideharu Ochiai¹, Kazunari Higa² and Hiroshi Fujise^{*1,2}

¹Institute of Biosciences, and ²Laboratory of Pathobiochemistry, School of Veterinary Medicine, Azabu University, 1-17-71 Fuchinobe, Sagami-hara, Kanagawa 229-8501

Received September 5, 2003; accepted January 10, 2004

KCC1 cDNA was cloned in dog erythroblasts that had differentiated from peripheral mononuclear cells. The size of the cDNA was 3,258 bp, the same as in pigs, but 3 bp longer than in humans and rodents. The dog KCC1 cDNA encodes for 1,086 amino acid residues with a calculated molecular mass of 120 kDa. The 560 bp cDNA fragment from position 679 to 1,238 in the full length cDNA from the dog erythroblasts was 100% identical to that in the kidney. Hydropathy analysis showed that the structure of dog KCC1 was similar to in other species; 12 trans membrane domains, four glycosylation sites in loop 5, and 17 consensus phosphorylation sites in the cytosol. However, there were variations in dog KCC1 compared to in other species; there was one CK2 phosphorylation site that was found only in dog KCC1. There were also substitutions of amino acids that affect pH sensitivity (His) and change acidic/basic residues or charged residues. In HEK 293 cells transfected with dog KCC1 cDNA (HEK-dKCC1), the Rb influx, which was ouabain-resistant, Cl-dependent, N-ethyl maleimide (NEM)-stimulative and Na-independent, was measured as for K-Cl cotransport, and the influx was found to be increased ~3 fold in HEK-dKCC1 compared to in the control. This ouabain-resistant Cl-dependent Rb influx was also volume-sensitive in hyposmotic medium, and the volume-sensitive component was inhibited by furosemide. Thus, the KCC1 cDNA cloned in dog erythroblasts encodes a volume-sensitive K-Cl cotransporter.

Key words: dog, erythrocyte, KCC1, K-Cl cotransport, Rb influx.

Abbreviations: CK2, casein kinase 2; dKCC1, dog KCC1; HEK-dKCC1, HEK293 cells transfected with dKCC1 cDNA; HEK-Vec, HEK293 cells transfected with vector; HK, high K; IMDM, Iscove's modified Dulbecco's medium; LK, low K; LP, loop; NEM, N-ethyl maleimide; NMDG, N-methyl-D-glucamine; PKA, protein kinase A; PKC, protein kinase C; RBCs, red blood cells; RVD, regulatory volume decrease; NKCC, Na-K-Cl cotransporter; TM, transmembrane domain.

K-Cl cotransport has been exploited for the regulatory volume decrease (RVD) in epithelial, endothelial and red blood cells (RBCs) (1–3), and the role of cell volume regulation was intensively examined in RBCs (3–5). In human RBCs, K-Cl cotransport activity is very low or latent in normal mature RBCs, but elevated in erythroblasts (5, 6). Thus, K-Cl cotransport was considered to be one of the critical systems for RVD during the differentiation of erythroid progenitor cells (4). The K-Cl cotransport was also elevated in sickle cells, and the cotransport might cause dehydration in these cells. Thus, regulation of K-Cl cotransport has been attempted to prevent sickle cell dehydration (7, 8). This volume-sensitive K-Cl cotransport in RBCs has been evaluated in many species of dog, sheep, pigs, horses, as well as humans. The K-Cl cotransport activities and the responses to modulators vary among these species (4), presumably due to the variation in the molecular events of either K-Cl cotransporter (KCC) or the regulation cascade among animal species.

In mutant dog RBCs in which the Na, K-pump remained and the cellular potassium concentration was

high (HK), K-Cl cotransport was measured under physiological ion conditions and it exerted for RVD (9, 10). In the HK RBCs, the K-Cl cotransport activity in 10% of young cells was 8-fold higher compared to that in 10% of old cells, and the RVD ability of young cells was also higher than in old cells. The volume of HK RBCs increased during cell aging in the circulation because of the decrease in the abilities as to K-Cl cotransport and RVD, though the cell volume of normal dog RBCs in which the cation composition involves low K and high Na (LK) decreased during aging (11). Thus, the decrease in K-Cl cotransport activity caused an increase in the cell volume in the HK dog RBCs, and there might be some defect in the K-Cl cotransport and RVD in these HK cells.

Several keys for elucidating the regulation mechanism for K-Cl cotransport were evaluated; phosphorylation/dephosphorylation and the redox system (12–14). However, the whole regulation mechanism remained unclear. Chemical modification of the regulation system is not simple; it might occur in both the cotransporter itself and the regulation cascade. It was not until Gillen *et al.* cloned the cotransporter in man, rabbit and rat in 1996 that molecular identification of the cotransporter was accomplished, leading to a better understanding of the mechanism of K-Cl cotransport (15). KCC is encoded by the KCC1 gene, and which is a member of a large cation-

*To whom correspondence should be addressed. Tel/Fax: +81-42-769-1629, E-mail: Fujise@azabu-u.ac.jp

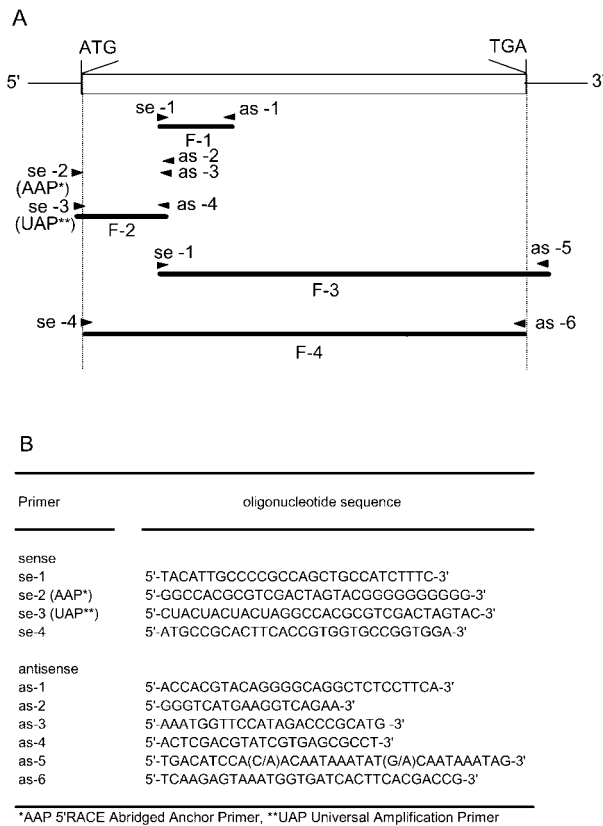


Fig. 1. Location of nucleotide primers for PCR/RACE of dog KCC1 (dKCC1) cDNA and the fractions generated on the PCR (A), and the sequences of sense (se) and antisense (as) oligonucleotide primers for PCR/RACE (B).

chloride cotransporter family (16–18). Following this discovery, several reports explained the mechanism of K-Cl cotransport according to the results of analysis of the molecular structure (19–23). In erythroblasts that had differentiated from erythroleukemia cells, KCC1 cDNA was cloned in man and mouse, and the existence of the mRNA and protein of KCC1 was confirmed.

As mentioned above, the characteristics of dog K-Cl cotransport activity were unique, given the dimorphism in HK and LK, and the sudden decreases in the abilities as to K-Cl cotransport and RVD during aging in the HK RBCs, but not in LK RBCs. Thus, molecular identification of dog KCC1 may provide possible clues to explain the mechanism. Here we report the cloning and expression of KCC1 from erythroid progenitor cells in dogs that had differentiated from peripheral mononuclear cells.

MATERIALS AND METHODS

Animals—Peripheral blood and a kidney tissue were obtained from a Japanese Shiba dog possessing RBCs with LK and HK (24, 25). All experiments were performed according to the guidelines of The Laboratory Animal Care Committee of Azabu University, and complied in The Japanese Animal Welfare Guide.

Isolation of Progenitors of Red Blood Cells—The progenitors of red blood cells, mostly erythroblasts, were prepared as reported elsewhere (26, 27). In brief, mono-

nuclear cells from LK and HK dogs were separated by Percoll gradient density centrifugation from the peripheral blood, and then the cells were incubated in Iscove's modified Dulbecco's medium (IMDM, Gibco BRL) with 10% fetal calf serum and 5% phytohemagglutinin-stimulated leukocyte conditioned medium at 37°C under an atmosphere containing 5% CO₂ for 7 days. On day 7, phagocytic cells were removed by the carbonyl iron method, and non-phagocytic cells were then cultured in IMDM medium supplemented with 30% FCS, 1% deionized bovine serum albumin, 300 µg/ml iron-saturated transferrin and 2U/ml recombinant erythropoietin (PBL Biomedical Laboratories) at 37°C under an atmosphere containing 5% CO₂ and 5% O₂. The cells were harvested during the second culture with erythropoietin, and then allowed to differentiate into mostly erythroblasts; 60% and 90% of the cells were hemoglobin-positive on days 3 and 6, respectively.

RNA Isolation and RT-PCR—All RNA was extracted from the erythroblasts and kidney tissue according to the acid guanidinium thiocyanate-phenol-chloroform method. First-strand cDNA was synthesized using a Superscript Pre-amplification System (Gibco BRL) with random hexamers, the cDNA serving as a template to generate fragments and full-length KCC1-cDNA. The PCR primers used are indicated in Fig. 1.

First, a cDNA fragment of KCC1 was amplified with primers designed according to the human, rabbit and rat KCC1 sequences (15): se-1 and as-1 as sense and antisense primers, respectively. PCR was performed using Ampli-taq DNA polymerase (Applied Biosystems) for 40 cycles of 94°C for 30 s/60°C for 12 s/72°C for 90 s, and the products were examined by electrophoresis. To determine the sequence of the 5' cDNA end, 5'RACE was performed using a 5'RACE System (Gibco BRL) and gene-specific primers (as-2, 3 and 4). The sequence of the 3' cDNA end was determined with PCR with primers se-1 and as-5. To generate the full-length dog KCC1 (dKCC1)-cDNA, finally a long and accurate PCR was performed with an Expand High Fidelity PCR System (Boehringer Mannheim) with primers se-4 and as-6.

Cloning and Sequencing of dKCC1—The fraction of the gel containing the amplified cDNA was excised and purified. The cDNA was ligated into the pCRII-TOPO plasmid (Invitrogen), and the plasmid was transformed into competent *Escherichia coli* cells. The cloned cDNA was sequenced with an automated sequencing machine (DSQ-1000L, Shimadzu, Tokyo) with a fluorescent labeled primer cycle sequencing kit (Amersham Pharmacia Biotech). The cDNA sequence was examined by assessment of the nucleotide sequences of mammals stored in the GenBank with the assistance of a computer program (Genetyx-Mac). Hydropathy analysis of the deduced amino acid sequence of dKCC1 was also conducted using this computer program according to Kyte and Doolittle (28).

Transfection of dKCC1 into HEK293 Cells—The c-Myc epitope-tagged dKCC1 cDNA expression vector was produced as reported (15). In brief, the sequence of the c-Myc epitope-tag was added next to the start codon (ATG) of the dKCC1 cDNA by PCR, followed by subcloning into the pcDNA3.1 mammalian expression vector (Invitrogen). The dKCC1 expression vector was transfected into

HEK293 cells (HEK-dKCC1) by the calcium phosphate method. HEK293 cells were also transfected with only vector pcDNA3.1 (HEK-Vec). At 24 hours after transfection, the cells were treated with trypsin, transferred to a poly-D-lysine coated 24-well plate at a density of 5×10^5 cells/well, and then incubated for another 24 h.

Rb Influx in HEK293 Cells—Rb influx was measured in HEK-dKCC1 and HEK-Vec cells as described elsewhere (15, 21). The cells were washed once with an isotonic solution comprising (in mM) 130 NaCl (or Na-sulfamate), 5 KCl (or K-sulfamate), 2 CaCl₂ (or Ca gluconate), 1 MgCl₂ (or Mg gluconate), 10 glucose, 0.1 ouabain, 0.1% BSA, and 20 HEPES/Tris, pH 7.4 at 37°C. The cells were then treated with 0.2 mM *N*-ethyl maleimide (NEM) for 10 min in the above solution, and washed three times with an Na-free medium comprising 130 *N*-methyl-D-glucamine (NMDG)-Cl (or NMDG-sulfamate), 5 KCl (or K-sulfamate), 2 CaCl₂ (or Ca gluconate), 1 MgCl₂ (or Mg gluconate), 10 glucose, 0.1 ouabain, 0.1% BSA, and 20 HEPES/Tris, pH 7.4 at 37°C. To avoid the contribution of the Na/K pump- and Na-K-Cl cotransporter (NKCC)-mediated Rb fluxes, 0.1 mM ouabain was added and Na was substituted with NMDG in the medium, respectively. Thereafter, Rb uptake was measured using a flux medium containing 25 mM RbCl (or Rb-sulfamate). To examine furosemide sensitivity, the Rb uptake was measured in the medium with or without 2 mM furosemide. For the measurement of volume-sensitive Cl-dependent Rb influx, instead of treatment with NEM, a hyposmotic medium (150 mOsm) was used as the flux medium in which the concentration of NMDG-Cl (or NMDG-sulfamate) was reduced. As a tracer, ⁸⁶RbCl (444 kbq/ml, Amersham Pharmacia Biotech) was used. Rb uptake was terminated at several time points by washing with ice-cold phosphate-buffered saline. After solubilizing the cells with 1% SDS, the radioactivity was measured with a liquid scintillation counter and the protein content was determined by the Micro BCA method (Pierce). Rb uptake was expressed as nmol/mg protein. Cl-dependent Rb uptake was calculated by subtraction of the uptake in the sulfamate medium from that in the Cl medium.

Western Blot—Western blotting was carried out as described elsewhere (15) using an anti-c-Myc antibody (Santa Cruz Biotechnology). The HEK-dKCC1 cells were homogenized with 250 mM sucrose, 1 mM EDTA, 10 mM Tris-HCl, pH 7.4, 100 µg/ml *p*-aminophenylmethylsulfonyl fluoride hydrochloride, 10 µg/ml leupeptin, and 2 µg/ml aprotinin, and then centrifuged. SDS-PAGE of the precipitate was performed using a 6% polyacrylamide gel. For deglycosylation, the sample was treated with *N*-glycosidase F (Roche). The protein bands in the gel were transferred to a polyvinylidene difluoride membrane, and then the membrane was treated with the primary antibody (mouse anti-c-Myc), and then the secondary antibody (horseradish peroxidase-linked mouse IgG). The c-Myc epitope tagged protein was detected with an ECL chemiluminescence detection system (Amersham Pharmacia Biotech) and exposed to an X-ray film.

Statistical Analysis—The Rb influx results were analyzed statistically using Student's *t*-test or Welch's *t*-test followed by the *F*-test. Differences were considered significant when *p* < 0.05.

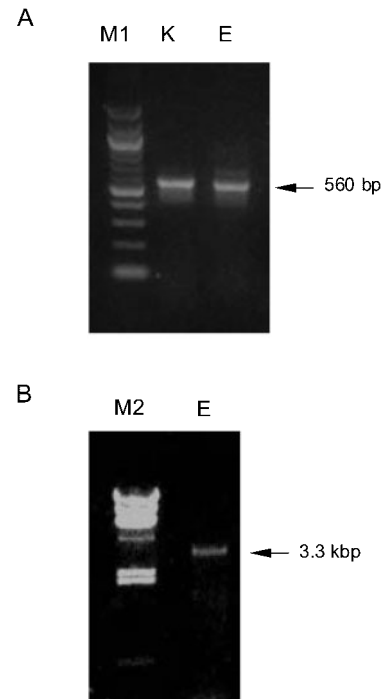


Fig. 2. Electrophoresis of the cDNA fraction amplified by PCR with primers *se-1* and *as-1* in dog erythroid progenitor cells (E) and kidney tissue (K) (A), and the full-length cDNA of the coding region of dKCC1 amplified by PCR with primers *se-4* and *as-6* in the erythroid progenitor cells (B). M1, 100 bp DNA ladder; M2, λ DNA-*Hind*III digest.

RESULTS

Figure 2 shows electrophoresis of the RT-PCR products of a fragment (560 bp) and the full-length KCC1 (*ca.* 3.3 kbp) cDNA from the erythroid progenitor cells, and a fragment from dog kidney. Firstly, the product of 560 bp cDNA (F-1 in Fig. 1A) was amplified in the erythroid progenitor cells and kidney by PCR. The amplified cDNA fragment was 87–89% identical to the KCC1 fragment at corresponding positions in the other species, and the homology of the sequences of the fraction was around 85–89% among the species reported. Thus, the cDNA fraction cloned in dog samples could be that of dKCC1. After determination of the 5'- and 3'-end regions of the dog-specific cDNA (F2 and F3 in Fig. 1A), the full-length dKCC1 cDNA was amplified by PCR using the dog specific primers in the erythroid progenitor cells (F-4 in Fig. 1A, and Fig. 2B).

The size of the full-length cDNA of dKCC1 from dog erythroid progenitor cells was 3,258 bp, the same as in pigs, but 3 bp longer than in humans, rabbits, rats and mice. The dKCC1 cDNA was cloned in both the LK and HK dog erythroid progenitor cells, and there were no differences in the sequence between these two cell groups. The cDNA sequence of the 560 bp fragment (F-1) generated from the kidney was 100% identical with the corresponding region in the erythroid progenitor cells from positions 679 to 1,238 in the cDNA sequence. The nucleotide sequence data reported here have been deposited in the DDBJ database under accession number AB011372.

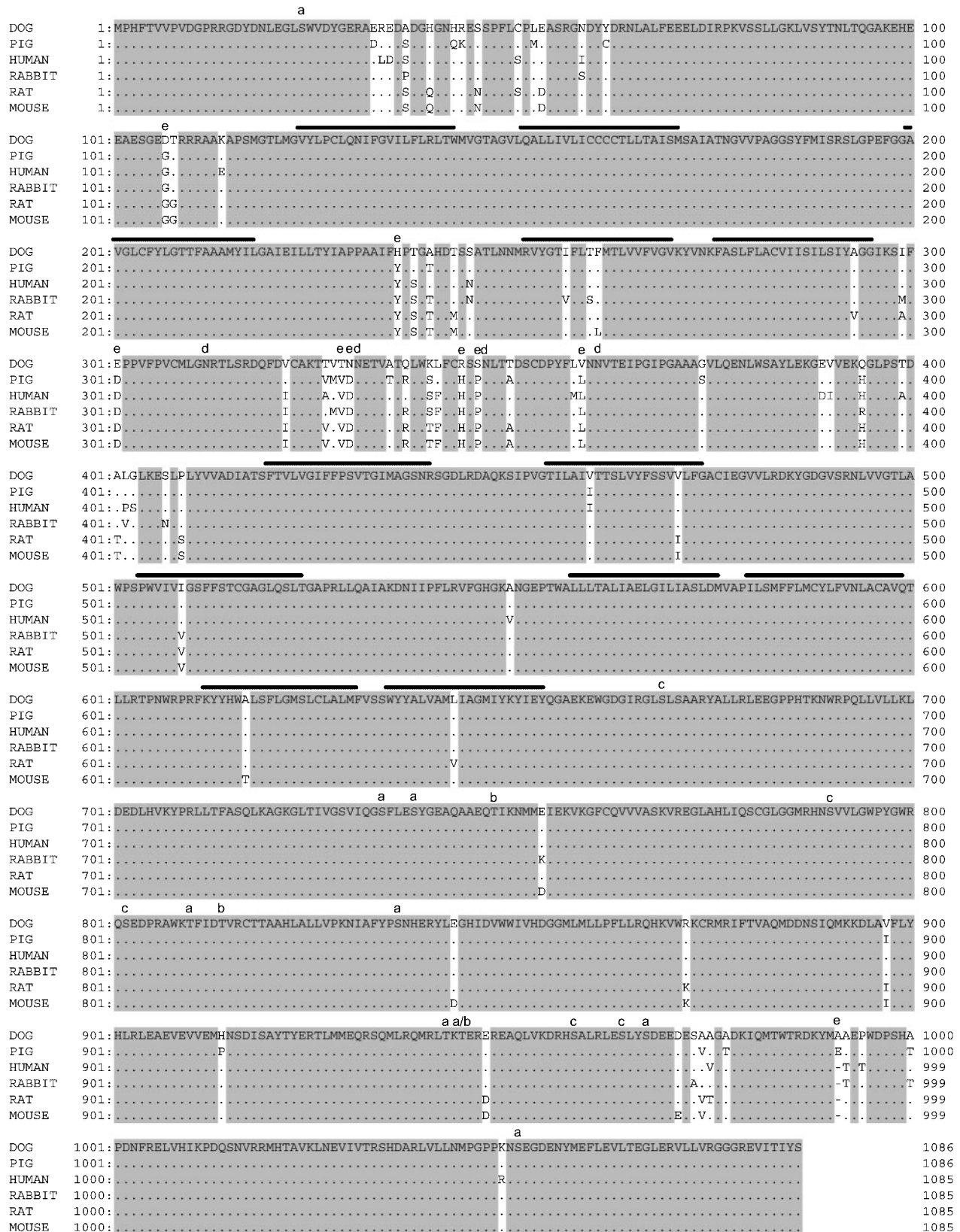


Fig. 3. Comparison of the deduced amino acid sequences of KCC1s from dog and other species reported. Transmembrane domains are overlined. a, b and c represent consensus phosphorylation sites for CK2, PKC and PKA, respectively; d, consensus glycosylation sites; e, amino acids only replaced in dog KCC1; shadowing, amino acids conserved among species.

		Amino acid					
		dog	pig	rabbit	human	rat	mouse
Nucleotide	dog		97	97	97	97	97
	pig	92		97	97	97	97
	rabbit	91	91		97	97	97
	human	91	91	92		97	96
	rat	90	89	89	89		99
	mouse	89	90	89	89	95	

Fig. 4. Comparison of the homologies in the cDNA and deduced amino acid sequences of KCC1 among dog, pig, rabbit, man, rat and mouse.

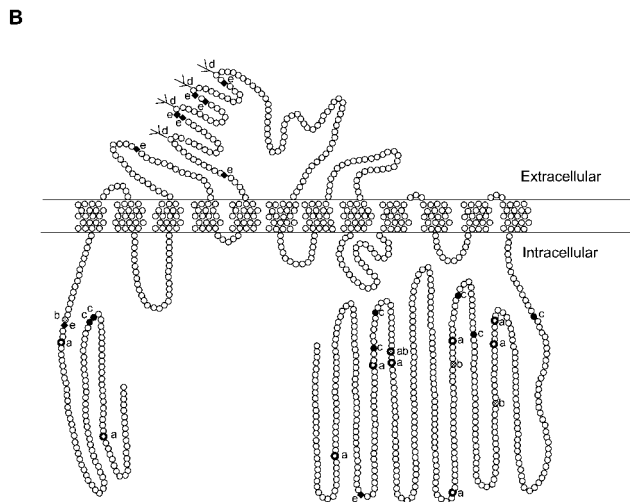
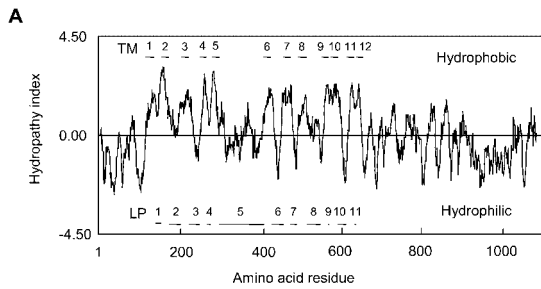


Fig. 5. Hydropathy analysis according to the method of Kyte and Doolittle (A), and the predicted transmembrane topology (B) of the deduced amino acid sequence of dKCC1 in dog erythroid progenitor cells. The transmembrane domains (TM) and loop domains (LP) are numbered in A. a, b and c represent consensus phosphorylation sites for CK2, PKC and PKA, respectively; d, consensus glycosylation sites; e, amino acids replaced only in dKCC1.

The dKCC1 cDNA encodes 1,086 residues of amino acids with a calculated molecular mass of 120 kDa. Figure 3 shows a comparison of the deduced amino acid sequences of KCC1s in the dog and other species reported. In the amino acid sequence of dKCC1, one amino acid insertion at position 991 was found compared

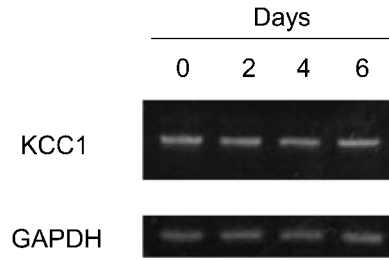


Fig. 6. Electrophoresis of the dKCC1 fragment amplified by RT-PCR in dog erythroid progenitor cells harvested on days 0 to 6 after adding erythropoietin. RT-PCR of glyceraldehyde-3-phosphate dehydrogenase (GAPDH) in the dog erythroid progenitor cells shown as control.

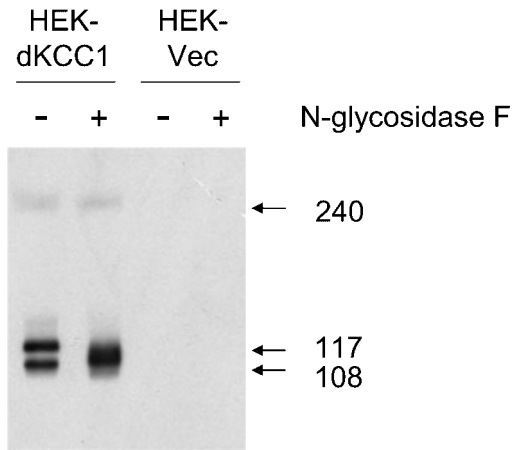


Fig. 7. Western blotting of dKCC1 in HEK293 cells transfected with dKCC1 (HEK-dKCC1) and the vector (HEK-Vec) after treatment with (+) or without (-) N-glycosidase F.

to that in humans and rodents. Fig. 4 shows a comparison of the cDNA and deduced amino acid sequences in the dog and other species reported (15, 17, 18). The cDNA sequences in these species were very similar, 89 to 95%, and the homology of the deduced amino acid sequences among these species was also high (96–99%).

Figure 5 shows the results of hydropathy analysis (A) and predicted membrane topology model (B) for dKCC1. The topology model was drawn according to the results of hydropathy analysis and previous reports (18). The hydropathy analysis pattern was almost the same for the species reported. There were 12 transmembrane domains (TM, numbered in Fig. 5A), 11 loops (LP, numbered in Fig. 5A) between the two TMs, and the N- and C-terminal domains in the cytosol. dKCC1 contained consensus 12 casein kinase 2 (CK2) and 5 protein kinase C (PKC) phosphorylation sites in the entire amino acid sequence: serine/threonine at positions 24, 104, 298, 329, 734, 738, 810, 836, 942, 944, 967 and 1051, and serine/threonine at positions 108, 438, 748, 814 and 944. The locations of these phosphorylation sites in the cytosol are shown in Fig. 5B. Twelve of the sites were conserved in all species reported (Fig. 3). One CK2 phosphorylation site was observed only in dog KCC1: serine at position 104. As cAMP-dependent protein kinase (PKA) phosphorylation sites that were located in the cytosol, three RXS and four

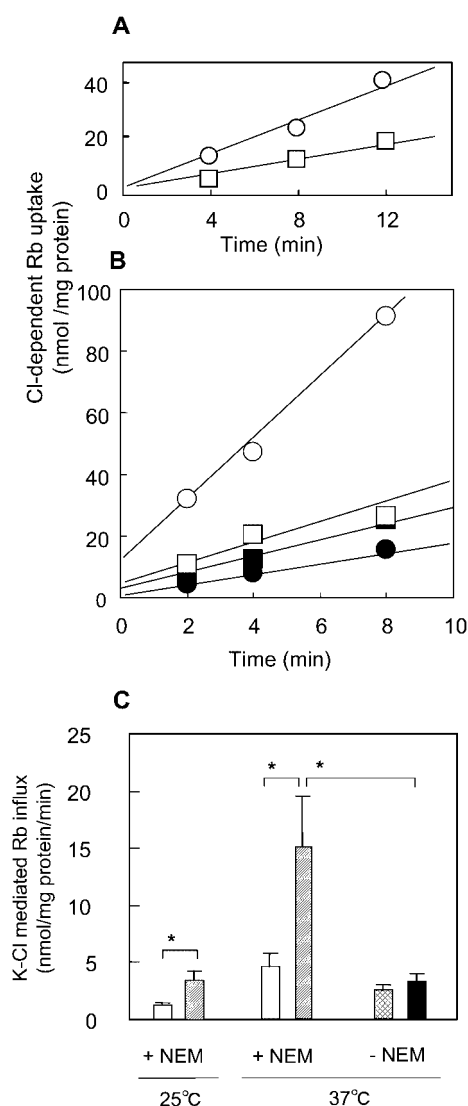


Fig. 8. Time course of ouabain-resistant, Cl-dependent (K-Cl-mediated) and NEM-stimulated Rb uptake (K-Cl-mediated Rb influx) in HEK-dKCC1 (open circles) and HEK-Vec (open squares) cells at 25°C (A) or 37°C (B), respectively, and the K-Cl mediated Rb influx in the HEK-dKCC1 (hatched columns) or HEK-Vec (open columns) cells at 25°C or 37°C (C). Ouabain-resistant Cl-dependent Rb uptake (B) and the influx (C) in the medium without NEM in HEK-dKCC1 (closed squares and cross-hatched columns) and HEK-Vec (closed circles and columns) cells at 37°C are also indicated. The values are typical of 5 to 6 similar experiments in A and B, and the means and SD of 5 to 6 individual experiments in C. *Statistically significant ($p < 0.05$).

RXXS sites were found: the former at positions 46, 802 and 958, and the latter at positions 47, 669, 790 and 964. Among them 5 PKA sites were conserved in all species reported. Four glycosylation sites at LP 4 were found to be conserved among the species reported: asparagines at positions 312, 331, 347 and 361.

Figure 6 shows the detection of the fragment of dKCC1 cDNA on RT-PCR in the erythroid progenitor cells harvested on days 0 to 6 after the addition of erythropoietin. The cDNA fragment was detected even on day 0 before the addition of erythropoietin, and it lasted until day 6

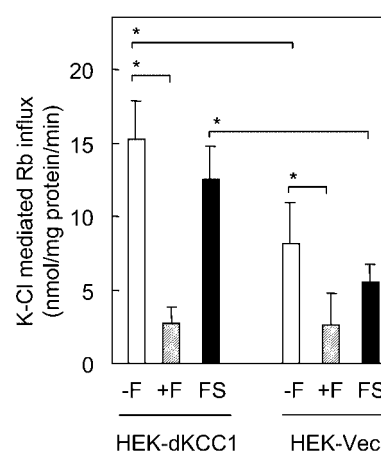


Fig. 9. K-Cl-mediated Rb influx in HEK-dKCC1 and HEK-Vec cells in the presence (+F, hatched columns) or absence (-F, open columns) of 2 mM furosemide. FS represents furosemide-sensitive influx (closed columns). The values are means and SD of 5 to 6 individual experiments. *Statistically significant ($p < 0.05$).

when almost all cells had differentiated into erythroblasts. Thus, the mRNA of dKCC1 was expressed at all stages of erythroid differentiation, even at the stage before the addition of erythropoietin. The expression levels of both dKCC1 and GAPDH did not change during the differentiation.

Figure 7 shows Western blotting of the dKCC1 protein in HEK-dKCC1 cells. The bands at 117 kDa and 108 kDa were found for HEK-dKCC1 but not for HEK-Vec cells. The 117 kDa polypeptide decreased in size on incubation with *N*-glycosidase F, comigrating with the 108 kDa polypeptide. Additionally, a band at 240 kDa was weakly detected for HEK-dKCC1 cells: this molecular mass matching that of the dimer of KCC1. Thus, the dKCC1 protein was expressed in HEK-dKCC1 cells.

The ouabain-resistant Rb uptake in the Na-free medium in which Cl was the main anion was greater than that in the medium in which sulfamate was the main anion in HEK-dKCC1 and HEK-Vec cells. In Fig. 8, the K-Cl cotransport mediated (K-Cl mediated) Rb uptake and the influx are shown. The K-Cl-mediated Rb influx at 37°C was decreased by 72% and 44% in the medium without NEM for HEK-dKCC1 and HEK-Vec cells, respectively. Thus, the NEM-stimulative Cl-dependent Rb uptake was measured as K-Cl-mediated Rb uptake. The K-Cl-mediated Rb uptake was linear at the measurement time points, both at 25°C and 37°C. At 25°C, the K-Cl mediated Rb influx in the HEK-dKCC1 and HEK-Vec cells were 3.36 ± 0.54 and 1.26 ± 0.31 nmol/mg protein/min, respectively, and those at 37°C were 14.2 ± 4.9 and 4.6 ± 1.5 nmol/mg protein/min, respectively. Thus, the K-Cl mediated Rb influx was enhanced in HEK-dKCC1 cells by 2.6- and 3-fold compared with in HEK-Vec ones at 25°C and 37°C, respectively. Figure 9 shows the effect of furosemide on the K-Cl-mediated Rb influx at 37°C. The influx was inhibited 82% and 67% by the addition of furosemide to HEK-dKCC1 and HEK-Vec cells, respectively.

Figure 10 shows the volume-sensitive, ouabain-resistant and Cl-dependent Rb influx in the medium without

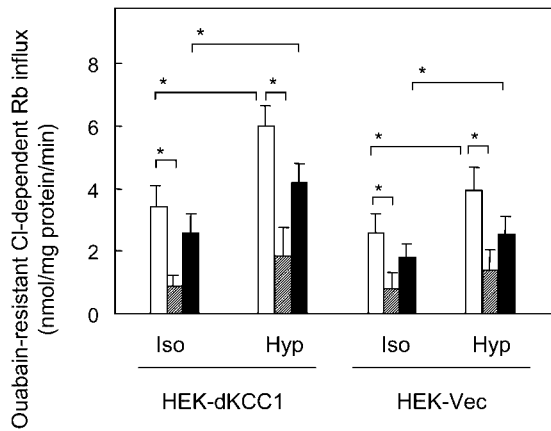


Fig. 10. Effects of hyposmotic medium and 2 mM furosemide on the ouabain-resistant Cl-dependent Rb influx in HEK-dKCC1 and HEK-Vec cells. Rb influx was measured in isosmotic (Iso, 295 mOsM) and hyposmotic (Hyp, 150 mOsM) medium in the presence (+F, hatched columns) or absence (-F, open columns) of 2 mM furosemide and also without NEM, and the furosemide-sensitive component was calculated (FS, filled columns). Values are means and SD of 5 to 6 individual experiments. *Statistically significant ($p < 0.05$).

NEM, and the effect of 2 mM furosemide on the Rb influx. The Rb influx in the hyposmotic medium was increased 1.8 and 1.7-fold, respectively, compared to that in the isosmotic medium in HEK-dKCC1 and HEK-Vec cells. The furosemide-sensitive component in the hyposmotic medium was 1.5-fold greater than that in the isosmotic medium in HEK-dKCC1 cells, though the component was not different in the isosmotic and hyposmotic medium in HEK-Vec cells. Thus, the furosemide-sensitive, ouabain-resistant and Cl-dependent Rb influx in the hyposmotic medium was mediated by K-Cl cotransport and was volume-sensitive.

DISCUSSION

Though the homology of the deduced amino acid sequences among species was very high (96–99%, Fig. 4), there were several clusters where the amino acid sequences differed among species: the clusters were located at the N-terminal, LP 3, LP 5 and C-terminal (Fig. 3). In the amino acid sequence, several amino acids were different only in the dog, compared with in other species, and the characteristics of several of these amino acids differed between dKCC1 and the other animal KCC1s. As to the pH effect on the transporter itself, His²³⁶ at LP 3 was replaced by Tyr, changing it into an amino acid possessing a pK_a of around physiological pH, and Arg³⁴⁴ at LP 5 was replaced by His, causing the loss of an amino acid with a pK_a of around physiological pH. In terms of changes of acidic/basic and charged amino acids, Asp¹⁰⁷ at the N-terminal was replaced by Gly, *i.e.* a change to an acidic or charged amino acid from a neutral one, and Lys³⁴⁰ at LP 5 was replaced by Ser, *i.e.* a change to a basic amino acid from a neutral one. These substitutions with amino acids with different characteristics may give an altered structure or function to the dKCC1 protein.

There was the possibility that dKCC1 might differ between HK and LK dog RBCs. However, the cDNA sequences for the LK and HK dog erythroid progenitor cells were identical. The abilities of K-Cl cotransport and RVD greatly decreased during cell aging in the circulation in the HK dog RBCs (11), and this result corresponded to that of Western blotting of RBCs in the mouse, in which the amount of the KCC1 polypeptide decreased with aging (23). The RVD system in normal LK dog RBCs comprises Na/Ca exchange transport, but it is K-Cl cotransport in the mutant HK dog RBCs. These RBCs could not employ the normal RVD system because of the change in intracellular cation composition, but the RVD in the HK RBCs used K-Cl cotransport that might have partially remained in the mature cells. Thus, there may be a RVD defect in HK RBCs, though KCC1 was not different between the HK and LK dog RBCs.

The bands of both non-glycosylated and glycosylated dKCC1 protein were detected on Western blotting in HEK-dKCC1 cells; thus, dKCC1 might be a glycosylated protein in the membrane. The molecular mass of 108 kDa for the non-glycosylated band was apparently smaller than the calculated molecular mass of 120 kDa. Su *et al.* also detected 108–130 kDa bands for rabbit and mouse KCC1 transfected HEK293 cells on Western blotting, though their calculated molecular masses without glycosylation were 120 kDa (23). In this experiment, such disagreement was also found. The molecular mass of a membrane protein calculated on electrophoresis has to be carefully analyzed. There is another possibility for this disagreement: the splicing form at the 3' end domain found in human KCC1 could not be examined with our PCR system (17), leaving the possibility that such a splicing form may exist in dog erythroblast KCC1.

The KCC1 protein was detected in RBCs from several species on Western blotting with anti-KCC1 peptide antibodies (23). However, the cloning of the full-length KCC1 cDNA from reticulocytes in humans failed, as only incomplete fragments were generated (17). The KCC1 polypeptide detected was increased in reticulocytes compared with in whole blood cells in the mouse, and the expression of the immunoreactive KCC1 in the young RBCs from β -thalasemia mice was 16-fold greater than that in the old cells (23). In dog erythroblasts that had differentiated from circulating mononuclear cells, KCC1 mRNA was detected at all stages in erythroid progenitor cells (Fig. 6). In the mouse, the expression of KCC1 mRNA was higher at the early stage in the erythroblasts compared with the later stage in the cells that had differentiated from mouse erythroid leukemia cells on Northern blotting, though the KCC1 cDNA fragment was detected on RT-PCR at all stages in the erythroid cells that had differentiated from ES cells (17, 23). The level for dKCC1 was obtained by RT-PCR in this experiment, and agreed with later results. This difference may be partly due to the methods employed; usually RT-PCR is much more sensitive than Northern blotting. KCC1 is ubiquitous in many tissues, though the expression level differs in several of them. Thus, the exact timing of the expression of KCC1 mRNA during erythroid maturation remains to be determined.

Erythroblasts are the terminal cells that lose their nuclei, so a sudden change in cell volume and other func-

tions may require KCC1 to maintain their cell volume. KCC1 might also have an important role in the differentiation stage or in high proliferation cells. In cervical cancer, the K-Cl cotransport activity and the expression of KCC1 mRNA became elevated as the malignancy increased (29). The cell volume of cervical malignant tumor cells was larger compared to that of normal cervical cells. Thus, K-Cl cotransport may exert its role in the cells that are going to change their cell volume during differentiation.

K-Cl cotransport seems to be regulated by several systems at the transporter itself and the regulation cascade, mainly through phosphorylation/dephosphorylation reactions and the redox system (1–4, 14). Though direct phosphorylation of the K-Cl cotransporter has not been demonstrated, it has consensus sites of phosphorylation by CK2, PKC and PKA. Inhibitors of phosphatase, okadaic acid and calyculin, caused a decrease in K-Cl cotransport activity, and an inhibitor of kinase, staurosporine, increased the activity (12–14). Several consensus phosphorylation sites located in the cytosol are conserved among species, implying that these consensus phosphorylation sites may be involved in regulation of K-Cl cotransport.

The cAMP response may be seen at early stages of erythroid development, though human RBCs could not respond to adrenergic stimuli due to the decrease in the adenylate cyclase system during erythroid cell maturation (30). Rat mature RBCs seem to be responsive to β -adrenergic stimulation, which causes an increase in intracellular cAMP, though adenylate cyclase activity and the number of β -receptors decreased during reticulocyte maturation (31, 32). In pig RBCs, intracellular cAMP stimulated K-Cl cotransport activity, though they failed to respond to β -adrenergic stimuli (33). These results may indicate that β -receptors and the following adenylate cyclase system are active in the early stage of erythroid maturation, but the system seems to disappear and remains of the system may exist at a later stage. Thus, cAMP probably acts as the regulator of the K-Cl cotransport either at the transporter itself or the regulation cascade in early-stage erythroid cells. Thus, there is the possibility that the PKA site(s) conserved among species are involved in the regulation of K-Cl cotransport, especially in the early stage of erythroid maturation.

As for the redox system, oxidizable agents cause an increase in the cotransport and reducing agents result in its decrease (4). Thiol and His in the cotransporter and regulation cascade, and glutathione and hemoglobin in the cytosol were considered the sites of action for the redox system (14). In oocytes transfected with mutant KCC1 in which the C-terminal domain was truncated or a neutral amino acid replaced by aspartate, the stimulation of K-Cl cotransport by NEM was abolished. There were 4 Cys and 16 His residues in the C-terminal domain. Some of these residues may thus be involved in the redox system.

There are three members of the cation-chloride cotransporter family: KCC, NKCC and Na-Cl cotransporter. In HEK293 cells transfected with KCC1, not only that of KCC, but also NKCC activity might be increased due to the change in intracellular Cl concentration (18, 34). Therefore, we had to carefully examine whether or

not the increased Cl-dependent Rb influx was mediated by KCC but not NKCC. To verify that the Cl-dependent Rb influx measured in this experiment was mediated by KCC, we employed Na-free medium: NMDG instead of Na was used as the main cation in the medium. There was additional evidence that the Rb influx was mediated by KCC but not NKCC: the K-Cl-mediated Rb influx increased on the addition of NEM, which is an inhibitor of NKCC (35). We therefore concluded that the ouabain-resistant, Cl-dependent, NEM stimulative, Na-independent and furosemide-sensitive Rb influx was mediated by KCC.

The volume-sensitive Rb influx, which was ouabain-resistant and Cl-dependent, increased in the medium without NEM in HEK-dKCC1 cells (Fig. 10). Thus, the flux might contribute to the regulatory volume decrease the same as in dog red blood cells (9–11). The volume decrease in the hyposmotic medium was measured only in the restricted conditions in HEK293 cells expressing human KCC1 (HEK-hKCC1); the volume decrease was measured with varying results in the medium in which the Cl concentration was reduced to 3 mM (34). The K-Cl cotransport in hyposmotic medium was increased 1.5 to 3-fold in several KCC1-transfected HEK293 cells (18, 34), though a recent report showed that there was no significant difference in the Cl-dependent component between KCC1-transfected HEK293 and control cells (21). Lauf *et al.* showed a huge increase of Cl-independent Rb influx in rabbit KCC1-transfected HEK293 cells in hyposmotic medium, and they suggested that K(Rb) exchange or channels might mask the K-Cl cotransport (21). Thus, to examine the volume regulation in more detail, a KCC1 expression model in which K(Rb) fluxes except that of KCC1 can be disregarded has to be established in the future. In the present experiment, we examined the volume-sensitive Rb influx for clues by examination of volume regulation in HEK-dKCC1 cells.

The K-Cl-mediated Rb influx was elevated in HEK-dKCC1 cells, so the function of KCC1 cloned from dog erythroid progenitor cells was confirmed. However, the stimulation by NEM was not so high in HEK-dKCC1 cells compared with in HK dog RBCs (36). The difference may be partly caused by the expression level of dKCC1 in HEK-dKCC1 cells. Several investigators have reported the stimulation of KCC1-mediated Rb influx on adding NEM to KCC1-transfected cells under different conditions. Though Lauf *et al.* showed stronger activation (6-fold) of the Rb influx in the medium with NEM at 37°C than at 23°C using Forbush's cell line, the effect of NEM was reported to be low in by others (15, 18, 21). Either the C-terminal domain in KCC1 (21) or the regulation cascade (14) might be the target(s) of NEM. Furthermore, the stimulation of Cl-dependent Rb influx was not clear on adding NO₂ in the HEK-dKCC1 cells (data not shown), while the stimulation was around 8-fold in the HK dog RBCs (11). Therefore, a target of NO₂ may exist at the regulation cascade in dog HK RBCs but not in HEK-dKCC1 cells. The large difference in the effect of NO₂ between HK dog and LK sheep RBCs may also mean that a target of NO₂ exists in the regulation cascade (37). These reasons may be the cause of the difference in the effect of NEM among the several KCC1-transfected cells.

In the present paper we report the molecular events for dog erythroid KCC1, and compared the similarity and differences in the KCC1 molecules and K-Cl cotransport activities among the species. Comparative analysis of the molecular structures and functions among species including dKCC1 may facilitate elucidation of the whole mechanism of KCC1.

This work was partly supported by a Grant in-Aid for Scientific Research from The Ministry of Education, Science, Sports and Culture of Japan (09660331), and funding from the Japanese Private School Promotion Foundation (1999, 2000) to HF.

REFERENCES

- Corcia, A. and Armstrong, W.M. (1983) KCl cotransport: a mechanism for basolateral chloride exit in *Necturus gallbladder*. *J. Membr. Biol.* **76**, 173–182
- Perry, P.B. and O'Neill, W.C. (1993) Swelling-activated K fluxes in vascular endothelial cells: volume regulation via K-Cl cotransport and K channels. *Amer. J. Physiol.* **265**, C763–769
- Cossins, A.R. and Gibson, J.S. (1997) Volume-sensitive transport systems and volume homeostasis in vertebrate red blood cells. *J. Exp. Biol.* **200**, 343–352
- Lauf, P.K., Bauer, J., Adragna, N.C., Fujise, H., Zade-Oppen, A.M., Ryu, K.H., and Delpire, E. (1992) Erythrocyte K-Cl cotransport: properties and regulation. *Amer. J. Physiol.* **263**, C917–932
- Hall, A.C. and Ellory, J.C. (1986) Evidence for the presence of volume-sensitive KCl transport in 'young' human red cells. *Biochim. Biophys. Acta* **858**, 317–320
- Dunham, P.B., Stewart, G.W., and Ellory, J.C. (1980) Chloride-activated passive potassium transport in human erythrocytes. *Proc. Natl Acad. Sci. USA* **77**, 1711–1715
- De Franceschi, L., Bachir, D., Galacteros, F., Tchernia, G., Cynober, T., Alper, S., Platt, O., Beuzard, Y., and Brugnara, C. (1997) Oral magnesium supplements reduce erythrocyte dehydration in patients with sickle cell disease. *J. Clin. Invest.* **100**, 1847–1852
- De Franceschi, L., Brugnara, C., and Beuzard, Y. (1997) Dietary magnesium supplementation ameliorates anemia in a mouse model of beta-thalassemia. *Blood* **90**, 1283–1290
- Fujise, H., Yamada, I., Masuda, M., Miyazawa, Y., Ogawa, E., and Takahashi, R. (1991) Several cation transporters and volume regulation in high-K dog red blood cells. *Amer. J. Physiol.* **260**, C589–597
- Fujise, H., Higa, K., Kanemaru, T., Fukuda, M., Adragna, N.C., and Lauf, P.K. (2001) GSH depletion, K-Cl cotransport and regulatory volume decrease in high K/high GSH dog red blood cells. *Amer. J. Physiol.* **281**, C2003–2009
- Fujise, H., Abe, K., Kamimura, M., and Ochiai, H. (1997) K⁺-Cl⁻ cotransport and volume regulation in the light and the dense fraction of high-K⁺ dog red blood cells. *Amer. J. Physiol.* **273**, R991–998
- Kaji, D.M. and Tsukitani, Y. (1991) Role of protein phosphatase in activation of KCl cotransport in human erythrocytes. *Amer. J. Physiol.* **260**, C176–180
- Cossins, A.R., Weaver, Y.R., Lykkeboe, G., and Nielsen, O.B. (1994) Role of protein phosphorylation in control of K flux pathways of trout red blood cells. *Amer. J. Physiol.* **267**, C1641–1650
- Lauf, P.K. and Adragna, N.C. (2000) K-Cl cotransport: properties and molecular mechanism. *Cell Physiol. Biochem.* **10**, 341–354
- Gillen, C.M., Brill, S., Payne, J.A., and Forbush III, B. (1996) Molecular cloning and functional expression of the K-Cl cotransporter from rabbit, rat, and human. A new member of the cation-chloride cotransporter family. *J. Biol. Chem.* **271**, 16237–16244
- Payne, J.A., Stevenson, T.J., and Donaldson, L.F. (1996) Molecular characterization of a putative K-Cl cotransporter in rat brain. A neuronal-specific isoform. *J. Biol. Chem.* **271**, 16245–16252
- Pellegrino, C.M., Rybicki, A.C., Musto, S., Nagel, R.L., and Schwartz, R.S. (1998) Molecular identification and expression of erythroid K:Cl cotransporter in human and mouse erythroleukemic cells. *Blood Cells Mol. Dis.* **24**, 31–40
- Holtzman, E.J., Kumar, S., Faaland, C.A., Warner, F., Logue, P.J., Erickson, S.J., Ricken, G., Waldman, J., Kumar, S., and Dunham, P.B. (1998) Cloning, characterization, and gene organization of K-Cl cotransporter from pig and human kidney and *C. elegans*. *Amer. J. Physiol.* **275**, F550–564
- Hiki, K., D'Andrea, R.J., Furze, J., Crawford, J., Woollatt, E., Sutherland, G.R., Vadas, M.A., and Gamble, J.R. (1999) Cloning, characterization, and chromosomal location of a novel human K⁺-Cl⁻ cotransporter. *J. Biol. Chem.* **274**, 10661–10667
- Mount, D.B., Mercado, A., Song, L., Xu, J., George, A., Jr., Delpire, E., and Gamba, G. (1999) Cloning and characterization of KCC3 and KCC4, new members of the cation-chloride cotransporter gene family. *J. Biol. Chem.*, **274**, 16355–16362
- Lauf, P.K., Zhang, J., Gagnon, K.B., Delpire, E., Fyffe, R.E., and Adragna, N.C. (2001) K-Cl cotransport: immunohistochemical and ion flux studies in human embryonic kidney (HEK293) cells transfected with full-length and C-terminal-domain-truncated KCC1 cDNAs. *Cell Physiol. Biochem.* **11**, 143–160
- Race, J.E., Makhlof, F.N., Logue, P.J., Wilson, F.H., Dunham, P.B., and Holtzman, E.J. (1999) Molecular cloning and functional characterization of KCC3, a new K-Cl cotransporter. *Amer. J. Physiol.* **277**, C1210–1219
- Su, W., Shmukler, B.E., Chernova, M.N., Stuart-Tilley, A.K., de Franceschi, L., Brugnara, C., and Alper, S.L. (1999) Mouse K-Cl cotransporter KCC1: cloning, mapping, pathological expression, and functional regulation. *Amer. J. Physiol.* **277**, C899–912
- Maede, Y., Amano, Y., Nishida, A., Murase, T., Sasaki, A., and Inaba, M. (1991) Hereditary high-potassium erythrocytes with high Na, K-ATPase activity in Japanese shiba dogs. *Res. Vet. Sci.* **50**, 123–125
- Fujise, H., Mori, M., Ogawa, E., and Maede, Y. (1993) Variant of canine erythrocytes with high potassium content and lack of glutathione accumulation. *Am. J. Vet. Res.* **54**, 602–606
- Wada, H., Suda, T., Miura, Y., Kajii, E., Ikemoto, S., and Yawata, Y. (1990) Expression of major blood group antigens on human erythroid cells in a two phase liquid culture system. *Blood* **75**, 505–511
- Higa, K., Ochiai, H., and Fujise, H. (2000) Molecular cloning and expression of aquaporin 1 (AQP1) in dog kidney and erythroblasts. *Biochim. Biophys. Acta* **1463**, 374–382
- Kyte, J. and Doolittle, R.F. (1982) A simple method for displaying the hydropathic character of a protein. *J. Mol. Biol.* **157**, 105–132
- Shen, M.R., Chou, C.Y., and Ellory, J.C. (2000) Volume-sensitive KCl cotransport associated with human cervical carcinogenesis. *Pflugers Arch.* **440**, 751–760
- Rasmussen, H., Lake, W., and Allen, J.E. (1975) The effect of catecholamines and prostaglandins upon human and rat erythrocytes. *Biochim. Biophys. Acta* **411**, 63–73
- Charness, M.E., Bylund, D.B., Beckman, B.S., Hollenberg, M.D., and Snyder, S.H. (1976) Independent variation of beta-adrenergic receptor binding and catecholamine-stimulated adenylate cyclase activity in rat erythrocytes. *Life Sci.* **19**, 243–249
- Farfel, Z. and Cohen, Z. (1984) Adenylate cyclase in the maturing human reticulocyte: selective loss of the catalytic unit, but not of the receptor-cyclase coupling protein. *Eur. J. Clin. Invest.* **14**, 79–82
- Kim, H.D., Sergeant, S., Forte, L.R., Sohn, D.H., and Im, J.H. (1989) Activation of a Cl-dependent K flux by cAMP in pig red cells. *Amer. J. Physiol.* **256**, C772–778

34. Gillen, C.M. and Forbush III, B. (1999) Functional interaction of the K-Cl cotransporter (KCC1) with the Na-K-Cl cotransporter in HEK-293 cells. *Amer. J. Physiol.* **276**, C328–336
35. Haas, M.C. (1994) The Na-K-Cl cotransporters. *Amer. J. Physiol.* **267**, C869–885
36. Fujise, H., Nakayama, T., Iwase, N., Tsubota, T., and Komatsu T. (2003) Comparison of cation transport and regulatory volume decrease between red blood cells from japanese black bear and the dog. *Comp. Clin. Path.* **12**, 33–39
37. Adragna, N.C. and Lauf, P.K. (1998) Role of nitrite, a nitric oxide derivative, in K-Cl cotransport activation of low-potassium sheep red blood cells. *J. Membr. Biol.* **166**, 157–167